



Citation: Nguyen, T.T., Garrido Sanchis A., Pashley R.M. (2025) Enhanced Desalination in a Hot-Bubble Pilot Plant. *Substantia* 9(2): 21-34. doi: 10.36253/Substantia-3353

Received: Feb 27, 2024

Revised: Jun 17, 2025

Just Accepted Online: Jun 19, 2025

Published: Sep 15, 2025

Copyright: © 2025 Nguyen, T.T., Garrido Sanchis A., Pashley R.M. This is an open access, peer-reviewed article published by Firenze University Press (<http://www.fupress.com/substantia>) and distributed under the terms of the Creative Commons Attribution License, which permits unrestricted use, distribution, and reproduction in any medium, provided the original author and source are credited.

Data Availability Statement: All relevant data are within the paper and its Supporting Information files.

Competing Interests: The Author(s) declare(s) no conflict of interest.

Research Article

Enhanced Desalination in a Hot-Bubble Pilot Plant

THI THUY NGUYEN*, ADRIAN GARRIDO SANCHIS AND RICHARD M. PASHLEY

School of Science, UNSW Canberra, Northcott Drive, Canberra, ACT 2610, Australia

* Corresponding author email: thi_thuy.nguyen@unsw.edu.au

Abstract. The bubble-column evaporator (BCE) offers a simple, energy-efficient and affordable seawater desalination process based on sub-boiling evaporation by enhancing the efficiency of heat and mass transfer through a constant flow of dense, heated bubbles rising in a solution-filled column. A large-scale hot-bubble pilot plant (HBPP), based on the BCE, was built to implement the thermal desalination process. Several different inlet gases, dry air, helium and combustion exhaust gas, were used in the HBPP to produce purified water from synthetic seawater. The efficiency was improved by using hot combustion gas instead of dry air or helium at the same inlet temperature, thereby reducing the energy consumption.

Keywords: Desalination, hot-bubble pilot plant, helium, combustion gas, dry air

1. INTRODUCTION

Seawater desalination has been widely used on a global scale to address freshwater scarcity resulting from rapid population and economic growth. Desalination techniques can be classified into thermal methods, which mostly involve heating water to its boiling point to generate water vapour, and high-pressure membrane processes in which seawater is filtered through a membrane¹. While membrane processes offer the advantage of separating salt from seawater without the need for high temperatures, they require comprehensive pre-treatment of the feedwater to avoid membrane fouling, together with the use of sophisticated energy-intensive high-pressure pumping systems². The main challenges in seawater desalination include achieving high efficiency, reducing energy consumption, preventing continuous membrane fouling in high-pressure membrane processes² and making the process more economical and environmentally acceptable³.

Bubble-column desalination is an innovative and emerging thermal technology that offers a simpler and more environmentally friendly process. The process is simpler because it does not require expensive membranes or a supply of high-pressure steam, enabling efficient heat and mass transfer at sub-boiling temperatures⁴. The bubble-column evaporator (BCE) is a scaled-down emulation of the natural semi-permeability of the water-gas interface

used for desalinating saltwater through a process resembling the water cycle^{3,4}. To be more specific, the BCE method uses a pre-heated inlet gas to transfer thermal energy to the aqueous solution, resulting in an efficient transfer of mass as water vapour into the rising bubbles created by the gas⁵. These bubbles quickly become saturated with the water vapour⁶ and transport it to the top of the column⁵, where it can be condensed into pure water⁷. The thickness of the water film through which the gas bubbles are sparged is of importance to both evaporation and condensation of the water vapour. However, the estimate of a thin heated solution layer surrounding the hot rising bubbles was developed in order to explain how salts like ammonium bicarbonate could be thermally decomposed at relatively low column solution temperatures⁸. That is because the AB ions cannot penetrate the bubbles, whereas viruses and bacterial cells could be exposed (at least their surfaces) to the hot gases in the bubbles and hence be sterilized⁹. With the bubble vapour desalination process, we are only interested in water vapour transfer across the gas/water interface and the energy requirement. Hence, the thickness of any heated water layer is not actually relevant to the bubble vapour desalination process.

The bubble column method makes use of a finding dating back to the 1930s, when Russian engineers observed that the introduction of salt into a flotation chamber led to a reduction in bubble size and an improvement in overall efficiency⁵. The presence of certain salts enhances the effectiveness of flotation by inhibiting bubble coalescence¹⁰; dissolved salt at seawater concentrations in the BCE process enables the formation in the column of a substantial packing volume of relatively uniform bubbles with diameters in the range 1–3 mm. This configuration significantly improves the efficiency of evaporation and transportation of saturated water vapour inside gas bubbles¹¹, as high density bubbles will collect water vapour throughout the entire body of the salt solution¹². By comparison, multistage flash distillation (MSF) uses essentially heating surfaces to flash evaporate water. Furthermore, the traditional thermal evaporation via boiling is an irregular process and can result in a higher rate of corrosion of the heating surfaces. In contrast, the BCE continuously produces new surfaces and the inhomogeneity in temperature between the bubbles and the solution catalyses transient high-temperature mass and heat transfer at temperatures significantly below boiling point with a high vapour-collection efficiency¹². Therefore, the bubble column method eliminates the need to boil the solution, thereby reducing inconsistencies and lack of control in the boiling process, and mitigating corrosion risks and scale production⁷. The continuous flow of

gas bubbles passing through the salt solution ensures controlled, uniform and very fast (a few tenths of a second) vapour collection up to saturation⁴.

Furthermore, water vapour, but not ions dissolved in the seawater, is continuously transported by the bubbles, so that the BCE process is resilient to highly contaminated feed solutions¹³, with no requirement for feedwater pre-treatment and no high pressures needed¹⁴. In contrast, commercial RO systems require high mechanical pressures significantly above the osmotic pressure of seawater to move pure water through a semi permeable membrane, in a relatively complicated process which produces large volumes of salt concentrate to be discarded out to sea.

Altogether, these factors contribute to an overall efficiency improvement, compared with quiescent systems⁴, making the dynamic bubble column method a promising approach for desalination. However, even though the bubble process is straightforward, our understanding of the physical and chemical principles underlying the BCE remains limited, leaving several aspects yet to be explored and fully elucidated¹⁵.

With the aim of enhancing the BCE process for desalinating seawater, several different inlet gases, air, nitrogen, carbon dioxide and helium, have been tried in a lab-scale BCE. Significantly enhanced evaporation occurred when using helium compared to dry air, an approximately threefold increase at an inlet-gas temperature of 150°C⁵. This was accompanied by a notable decrease in the apparent enthalpy associated with the vaporization of water ΔH_v ¹⁴.

These results were in good agreement with those reported by¹⁴ for inlet gases (air/helium) at 75°C. The evaporation efficiency with helium was about 3.1 times larger than with air, which indicates the promising potential application of operating a BCE with helium as the inlet gas, even at rather moderate temperatures. The helium could be heated by solar energy or waste vent gas. Rui Wei suggested that the fundamental principle underlying the improved evaporation efficiency with helium is the disruption of the hydrogen bonds in the water by the helium atoms¹⁴. Because of the relatively small molecular size of helium compared with the length of hydrogen bonds, helium atoms can penetrate the hydrogen-bond network and break up the bonds simply by atomic vibration¹⁴. However, accurate estimates of both efficiency and energy cost of the bubble desalination process with sparged helium flow could only be obtained by design and construction of a larger scale system, where the issues associated with vapour water condensation performance can be addressed. In the literature, there does not seem to be any useful follow-on work in papers citing Rui Wei's work. There-

fore, for the first time, this study aims to investigate the efficiency of the large-scale hot-bubble pilot plant (HBPP) based on the BCE for helium sparged aqueous salt solutions by comparing the condensation efficiency in a range of different input carrier gases (dry air, He and combustion exhaust gas). The new HBPP has been designed as a large-scale pilot test unit of a possible final commercial plant of BCE, where the issues associated with vapour condensation have been addressed.

Using dry air as carrier gas at an inlet temperature of 275°C to produce hot, dry bubbles has been investigated within a laboratory-scale BCE and resulted in a further 10% improvement in the effectiveness of water-vapour collection, suggesting that raising the inlet-gas temperature promotes increased vaporization¹⁶. Surprisingly, the rapid transfer of water vapour across the bubble surface, which occurs after hot, dry inlet air enters the column, did not have an impact on the inhibition of the coalescence of bubbles in salt solutions, compared with the prevention of water evaporation into the bubbles, using the vapour water saturated inlet air¹⁷. It appears that any local concentration enhancement in a thin region of solution around the bubbles, which produces soon after dry bubbles enter the column, has no influence on the film thinning process¹⁷. Another possibility is that both the bubbles and the solution flowing rapidly across the bubble's surface dissipate any significant solute concentration build up¹⁷. Whatever possible explanations for this could be, these lab-scale BCE processes demonstrated a higher energy efficiency, approximately 7.55 kWh/m³ of fresh water, compared with conventional thermal-desalination methods¹⁸. However, weighing the advantages and disadvantages of the use of dry air and humid air, the utilization of air with a certain level of humidity itself requires more energy to heat to a specific temperature, while it has no effect on the air bubble coalescence inhibition due to added salt, which is the basis for the bubble column method of desalination. Hence, optimizing operational factors, such as selecting dry air as an alternative inlet for humid air; using helium as the inlet gas rather than dry air and elevated inlet-gas temperatures would enhance the evaporation efficiency of the BCE process even further⁵ and reduce energy consumption^{14,18}.

The BCE method has recently been implemented in a hot-bubble pilot plant (HBPP) with the aim of developing an industrial-scale, energy-efficient water-treatment technology that increases evaporation efficiency while lowering energy usage¹⁹. In the first reported experiments, the HBPP used either hot air or hot combustion gases for water sterilization²⁰. There was a 37% increase in the evaporation efficiency at an inlet temperature of 120°C using the hot combustion gases, compared to

using air; this enhancement was partly ascribed to the heat that was generated when the water vapour in the combustion gas underwent condensation¹⁹. Furthermore, an analysis of the water condensed from the HBPP confirmed that it met the international standards for drinking-water quality¹⁶. Hence, incorporating exhaust gas from combustion processes into the large-scale HBPP is a promising method for seawater desalination with improved evaporation efficiency while producing high-quality condensed water. However, to examine whether there is an improvement in the condensation efficiency achieved in the large-scale pilot test unit, a study comparing the condensation performance of the bubble column desalination process when sparging combustion gas with that of other input carrier gases, including dry air and He is lacking.

Hence, this paper focuses on comparing the effectiveness of using dry air, helium or combustion gas as the inlet gas to optimize the working efficiency of the HBPP in desalinating seawater. The effect of different inlet-gas temperatures on the evaporation performance of the HBPP is also investigated using either helium or dry air.

2. MATERIALS AND METHODS

2.1. Experimental solution

HBPP was operated with a saline solution of known salt concentration to simulate seawater, rather than actual seawater, to ensure the evaporation experiments were conducted under controlled conditions. For each experiment, a solution of 0.5 M NaCl was prepared by adding 585 g of sodium chloride to 20 L of tap water. Tap water was used because the HBPP does not require pre-treatment of the feed solution. After the inlet gas was heated to its target temperatures of 90°C, 120°C, and 147°C, the experimental solution was poured into the solution chamber to initiate evaporation measurements.

2.2. Inlet gases

Experiments were first conducted using air or helium at different inlet gas temperatures, ranging from 90°C to 147°C. The amount of condensed water vapour collected every 5 minutes over a 60-minute period was used to evaluate the effect of inlet temperature on the efficiency of vapour transfer desalination. Subsequently, both air and helium were compared with combustion gas at the same flow rate and temperature. The number of moles of inlet gas per unit time was the same for all the inlet gases.

A 140 L/min flow of dry air at a temperature of 90°C was produced using two Hiblow HP 120 air blowers connected to a silica-gel desiccator (Fig. 1).

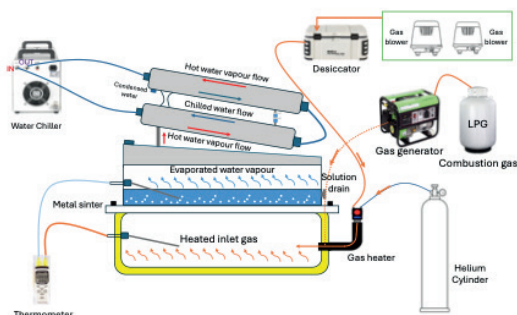


Figure 1. The HBPP setup for using different inlet gases (helium, combustion gas and air) (adapted from ¹⁹)

Dry helium was used directly from gas cylinders (Coregas; purity > 99.999%). The flow rate of dry helium was monitored by a rotary gas meter (FMR DN40 G016) and maintained at 140 L/min. Using dry helium carrier gas, the bubble column desalination process offers a higher overall mass and heat transfer compared with dry air (mentioned in the introduction), with less heat required for the dynamic heat-exchange process from the pre-heated inlet gas bubbles in evaporating the column solution due to its low heat capacity. Both the air and helium were heated by a Lesier LHS 21S gas heater and monitored with a thermometer (Tenmars TM-82N Type K/J).

The steady-state temperature of the column solution was measured at different inlet gas temperatures, after which the air and helium temperatures were adjusted to produce the same column solution equilibrium temperature (54°C) produced by 90°C combustion gas at a flow rate of 140 L/min. Here, we used liquid petroleum gas (LPG) as the combustible source without requiring additional heating equipment or gas pumps, which is emitted from biogas engines and is the byproduct of many industrial processes, such as pig farms, landfills, biogas power plants, and coal power plants. During combustion, the amount of air was carefully controlled to ensure that the LPG was fully combusted in a Green-power gas generator. The combustion exhaust flow then was connected to the gas chamber as the combustion gas inlet. By assuming that the LPG was a mixture of 50% (by mass) of butane (C_4H_{10}) and 50% propane (C_3H_8), the chemical formula of LPG was ($C_{3.5}H_9$). The composition of the combustion gas is the fully combusted products of the LPG and determined by equation (2). Hence, none of small fraction of unburned contaminants would end up in the water condensed from the HBPP.

Since the exhaust gas came with the combustion heat, heating helium that contains water vapor would require significantly more energy than using the combustion gas from the gas generator while as in the case of air, the presence of water vapor would not potentially enhance the system's performance. Hence, the current work introduced dry air and helium into the large-scale HBPP system to reduce the overall energy cost and scientifically determines the optimal operating conditions for the system's efficiency by a comparison with the efficiency of condensation using combustion exhaust gas.

2.3. Hot-bubble pilot plant

HBPP incorporated a metal sinter, and a gas chamber lined with high-performance refractory material. The 0.5 m² sinter, made from 316 stainless steel with Grade 40 porosity, maintained a continuous production of dense bubbles (1–3 mm in diameter). This size range ensured that the evaporated water vapour was completely saturated inside the rising bubbles by the time they reached the top of the column. A porous sinter was placed at the top of the gas chamber to continuously generate a stream of hot, dense, fine bubbles in the bubble column reactor, which transfer and collect heat and water vapour to and from the surrounding solution. Two thermocouples underneath and over the porous sinter monitored the inlet-gas temperature and the column-solution temperature. Figure 2 shows the internal structure of the HBPP.

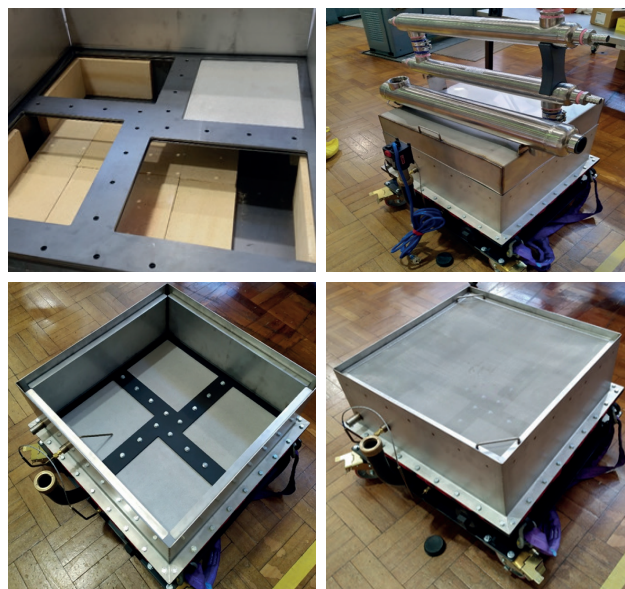


Figure 2. Structure of the HBPP. **Top left:** gas chamber with refractory material. **Top right:** condensing units. **Bottom left:** water-treatment column with the metal sinter. **Bottom right:** mesh cover (adapted from ²¹).

Insulating the gas chamber with refractory bricks significantly reduced thermal energy loss, thereby improving the pilot plant's performance. The service life of the sinter was prolonged by using heat-resistant material, effective even at temperatures greater than 500°C²².

The water-treatment reactor, with dimensions 500 mm × 500 mm × 250 mm, was placed on the top of the sinter and allowed for the treatment of up to 20 L of solution per batch operation. The solution height (250 mm) was designed to ensure that the ascending hot bubbles became fully saturated with water vapour before reaching the top of the reactor, thereby preventing contamination of the condensation units by foam generated during the process¹⁴. A mesh cover placed on top of the column further ensured that foam could not enter the condensing units.

The condensing units, which collected and condensed the water vapour (Fig. 2, top right picture), consisted of three interconnected shell-and-tube heat exchangers, providing a total surface area of 3m². Chilled water was circulated through each condensation unit, with an industrial water chiller (CW-5000AG) maintaining the water temperature at approximately 24°C. Once the desired inlet gas temperature was reached, 20 L of 0.5M NaCl solution was introduced into the water treatment reactor, marking the start of the experiment (time zero). Evaporation occurred at the surfaces of the hot rising gas bubbles, which ascended to the top of the reactor, where they collapsed and released water vapour that was then condensed. The volume of condensed water was measured every 5 minutes.

3. RESULTS AND DISCUSSION

3.1. Influence of inlet-gas temperature

In the current experiments, a continuous flow of hot, dry air or pure helium at varying inlet gas temperatures was used as a carrier gas in the open-to-atmosphere bubble chamber to evaporate water from concentrated salt solutions (0.5M). The effects of substantially increased gas-bubble temperatures on the efficiency of water vapour collection from the HBPP were examined. Shahid¹⁷ found that a significantly higher rate of evaporation was achieved by the use of high inlet-gas temperatures. The findings are consistent with the notion that a significant degree of supersaturation within the bubbles can be obtained at high bubble temperatures.

This is possibly due to the combined effects of high-temperature inlet gases and supersaturated conditions, which enhanced the performance of the BCE process for thermal desalination⁴ by increasing the rate of vapour

transfer²³. In fact, a continuous flow of hot, dry air bubbles at 275°C was used to improve the water vapour collection rate by approximately 10% compared to the vaporisation expected from equilibrium vapour pressures¹⁷. This study further confirms the enhanced desalination in the large-scale HBPP due to the positive effects of high bubble temperatures on the efficiency of vapour transfer.

Since the effect of increased inlet gas temperature on the intervening liquid film trapped between colliding bubbles is negligible within the range of 150–275°C^{17,23}, it may not play a critical role in preventing these bubbles from combining, even at temperatures below 150°C, as suggested by the film drainage model⁴. This suggests that local heating in the adjacent solution, caused by inlet gas temperatures below 150°C, does not significantly alter film viscosity and, therefore, does not clearly dominate the rate of vapour transfer.

Another way to assess the impact of high-temperature inlet gas on heat and mass transfer processes in desalination is through the bubble evaporation layer model⁴. In this model, the presence of a thin heated solution layer surrounding the hot rising bubbles is used to explain how the performance of BCE increases with increasing inlet-gas temperatures: water molecules are moved into the heated layer around the surface of the bubbles and hence carried away.

However, for desalination, the primary focus is on water-vapour transfer across the gas-water interface and the energy required for this process. The thickness of any heated water layer is not actually relevant to this process, although it is a function of steady-state column temperature⁴. In fact, the gas-water interface drives the evaporation process and transportation of saturated vapour, which produces drinking water from seawater in a continuous flow evaporative bubble column operating below the boiling point. This means that a higher surface area of the gas-water interface correlates with improved heat and mass transfer efficiency⁴.

Nonetheless, the heat from a hot, dry bubble entering the column is passed to the transient hot water layer surrounding its surface to cause water evaporation⁴. As the bubble approaches a steady state, the water film formed around the rising bubbles cools to the equilibrium temperature of the column solution when hotter bubbles flow into the HBPP. As a result, this hotter layer has a stronger influence on changes within the solution, particularly on water evaporation. Even if the same heated gas-water interfacial area is created with hotter gas bubbles, the higher heat transfer coefficients in the HBPP system enhance evaporation efficiency, while the column temperature remains well below the boil-

ing point⁴. This supports the view that enhanced water evaporation appears to increase with gas temperature, as shown in the following sections.

3.1.1 Air as the inlet gas

Figure 3 shows boxplots of the average volume of water collected every 5 minutes at different temperatures using air as the inlet gas.

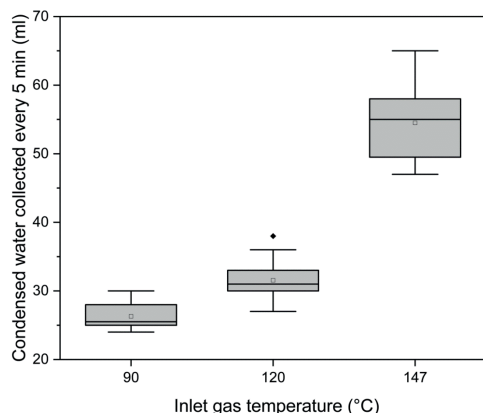


Figure 3. Average volume of condensed water collected every 5 minutes from the NaCl solution at different inlet-gas temperatures using air as the inlet gas.

The results show a clear trend: the volume of water collected increased as the inlet-air temperature increased in the range of 90–147°C (one factor ANOVA in SPSS; $F = 1256$; $df(5, 59)$; $p < 0.0001$; Dunnett T3 test, 95% CL). This indicates that evaporation is strongly dependent on inlet-air temperature. Moreover, since the efficiency continued to increase, the optimal inlet-air temperature must be higher than the highest temperature here, 147°C. At high inlet-gas temperatures, the HBPP exhibited strong desalination performance because of the rapid mass and heat transfer at the interface between the solution and the hot gas bubbles. When the inlet-air temperature rose, the temperature at this interface also increased; more heat was exchanged between the hot air bubbles and the surrounding solution to reach a new dynamic equilibrium, and the bubbles collected a greater volume of water vapour.

It should be noted that not all the heat supplied by the heated inlet air was transferred to the column to produce saturated vapour in the bubbles²³. Also, assuming perfect thermal insulation of the bubble column, the expected equilibrium temperature can be directly calculated from the inlet-gas temperature using the steady-

state thermal-energy balance equation developed in a bubble column (Equation 1 in ¹⁸). Hence, with the inlet air at higher temperatures, the column solution constantly attained a higher temperature than that expected at steady-state operating conditions²³. This led to a higher vapour transfer mass (as calculated from the observed column temperature) in comparison to the observed total transfer mass. However, it is interesting that, in all the experiments carried out with the inlet-air temperatures of 150–250°C, the observed vapour transfer was found to be higher than that expected for the column operating at steady-state conditions²³. These results suggest that, although the balance between the heat supplied and the heat required for vaporisation was not achieved at high inlet-air temperatures, an enhanced water transfer rate was still observed with increasing air temperature²³.

In the current study, the ‘expected’ rate of water vapour production was calculated by multiplying the saturated vapour density carried in an air bubble ($\rho_v(T_e)$ in g/m³; see Table 1) at equilibrium for every 5-minute interval of the 60-minute runs by the airflow rate in the water treatment column/reactor (140 L/min) over each 60-minute run²⁴.

Table 1. Expected and experimental water transfer rates comparison using HBPP for 60 min bubbling run with 140 L/min airflow rate (adapted from ⁵)

Inlet air temp. (°C)	Column solution temp. (°C)	Water vapour density (g/m ³) (adapted from Fig. 2 in ⁵)	Expected water vapour carryover (mL), A*	Measured volume of water evaporated (mL), B*
90	42.6	59.80	41.9	26.29
120	54.3	103.48	72.4	31.54
147	55.1	107.74	75.4	54.50

Across the range of inlet air temperatures from 90 to 147°C, the calculated water vapour carryover—measured from the point when stable water condensation performance was observed—was higher than the actual amount of condensed water produced by the BCE commercial prototype (Table 1). Therefore, while higher water transfer rates per unit volume of air into the rising bubbles were clearly achieved by increasing the inlet air temperatures (Table 1), due to the substantial increase in steady-state water vapour density data⁵, it is likely that full condensation of the water vapour was not achieved in this study. Additionally, heat loss from the hot inlet gas flow may not have been effectively prevented during the gas transmission process.

In earlier works, the bubble column was weighed to obtain the accurate water-vapour loss, indicating

that water was not condensed^{17,23}. For instance, increasing the temperature of air bubbles from 150 to 250°C raised the weight of water vapour removed from the aqueous NaCl solution from 6.2% to 8.3%, exceeding the expected water vapour carryover rate²³. Moreover, Shahid¹⁷ reported that a continuous flow of hot, dry air at 275°C resulted in approximately 10% higher water vapour collection efficiency than expected from equilibrium vapour pressures. However, in the current work, though condensation took place in the larger scale pilot test unit, the efficiency of water vapour collection was much less than expected, around 50 – 60 % of the expected amount (Table 1). This suggests that the condensation unit requires further optimization to increase the water-vapour saturation levels in the bubbles for sea-water desalination.

On the whole, although hot air bubbles at temperatures ranging from 90 to 147°C passing into the column at a flow rate of 140 L/min did not increase the water vaporisation over the expected volume of water evaporated at steady-state conditions, the initial results reported here still support the view that increasing the inlet-gas temperature further improves the water-vapour collection rate.

3.1.2 Helium as the inlet gas

It is well known that the equilibrium water-vapour density in bubbles of any gas is only a function of the liquid-water temperature and is independent of whether the solution is boiling or not¹⁹. In other words, the amount of equilibrated water vapour contained in the bubbles is the same as that collected in boiling bubbles at the same solution temperature¹⁴. Consequently, an increase in inlet gas temperature is expected to enhance the amount of water vapour carried by the bubbles for both air and helium¹⁷.

For this reason, the same setup was used for helium as for air, with the results in Fig. 4. When the helium temperature was increased from 90°C to 147°C, there was a significant and linear increase in the evaporation efficiency (one factor ANOVA in SPSS; $F = 731.8$; $df (2, 16)$; $p < 0.0001$; Dunnett T3 test, 95% CL). These findings are in agreement with those reported by^{19,23}, which show that, by increasing the inlet-gas temperature, the amount of condensed water vapour increased accordingly. Interestingly, despite the lower water vapour density with helium at 75°C¹⁴, the evaporation efficiency was similar to that observed with helium at 150°C⁵, due to its superior ability to disrupt hydrogen bonding among water molecule clusters¹⁴. Wei and Pashley¹⁴ found that at a heated helium inlet temperature of 75°C, the actu-

al solution weight loss measured by a balance over a 30-minute run was approximately 3.1 times higher than the expected loss, which was calculated by summing the evaporated water weight loss per minute based on the corresponding vapour pressure at the actual column solution temperature. Similarly, at a helium inlet temperature of 150°C, the actual weight loss measured was approximately 3.3 times higher than the theoretical weight loss⁵. These results indicate that when using helium as a carrier gas, variations in inlet temperature have a relatively minor impact on evaporation efficiency. This means that operating a BCE with moderately heated helium gas inlet can still significantly facilitate the evaporation efficiency¹⁴.

However, the results in Table 2 for helium obtained in the industrial-scale BCE, i.e. HBPP show that the amount of water evaporated in the bubble column reactor was only marginally higher than the calculated theoretical water-vaporisation rate based on the observed column temperature.

Table 2. Desalination efficiency with inlet helium temperature (adapted from ⁵).

Inlet helium temp. (°C)	Column solution temp. (°C)	Water vapour density (g/m ³)	Expected water vapour carryover (mL), A*	Measured volume of water evaporated (mL), B*	Vaporisation efficiency [B*/A*]
90	40.5	54.15	37.9	35.14	0.9
120	52.5	95.16	66.6	73.25	1.1
147	53.5	99.23	69.5	106.00	1.5

In particular, at an inlet gas temperature of 147°C, there was an observed increase of a factor of 1.5, which was the highest vaporisation efficiency among all the tested inlet temperatures. This value is significantly lower than the vaporisation efficiencies reported for the lab-scale BCE, where helium demonstrated 3.3 times higher efficiency than theoretical values⁵. Besides, helium was found to have 0.9 and 1.1 vaporisation efficiency at the lower temperatures of 90°C and 120°C, respectively.

In this calculation, it is important to note that vaporisation efficiency was determined by dividing the volume of evaporated water measured during the runs, B^* , by the expected water transfer value based on the actual column temperature, A^* . Table 2 presents the measured total volume transferred using hot helium bubbles at temperatures ranging from 90°C to 147°C B^* , and the expected volume at steady state A^* , at a flow rate of 140 L/min.

The significantly higher carryover of water vapour by helium gas observed by^{5,14} was not observed in this

BCE commercial prototype. This discrepancy may be attributed to the fact that the bubble column reactor was not well insulated with refractory material to control the heat loss of the hot inlet gas flow during the evaporation process. Also, the condensation system may be insufficient, resulting in incomplete condensation of the collected water vapour.

In conclusion, the initial experiments were conducted using the same flow rate and inlet temperature for both air and helium. However, different steady-state temperatures were observed in the column solution due to the differing heat capacities of helium and air, which affect heat transfer for solution evaporation at the same inlet temperatures. An increase in evaporation efficiency was observed with higher inlet gas temperatures for both gases, as shown in Figs 3 and 4.

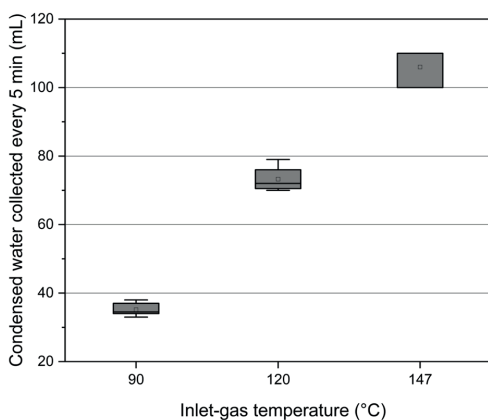


Figure 4. As for Fig. 3 but using helium as the inlet gas.

In subsequent experiments, the inlet-gas temperature was adjusted to achieve the same steady-state temperature in the column for both air and helium. This approach allowed for the use of the steady-state column solution temperature to estimate the expected water vapour carryover for each gas, facilitating a direct comparison of their performance.

3.2. Influence of inlet-gas type

3.2.1 Helium and air

Different gases exhibit varying evaporation efficiencies due to their distinct effects on the mass and heat exchange processes between the bubbles and the surrounding salt solution. The faster equilibrium was reached in the movement of water vapour into the bubbles, the quicker the bubbles saturated with water

vapour and the higher the evaporation efficiency. A comparison of the volumes of condensed water collected using air and helium as the inlet gas at an equilibrium temperature of 54°C is shown in Fig. 5.

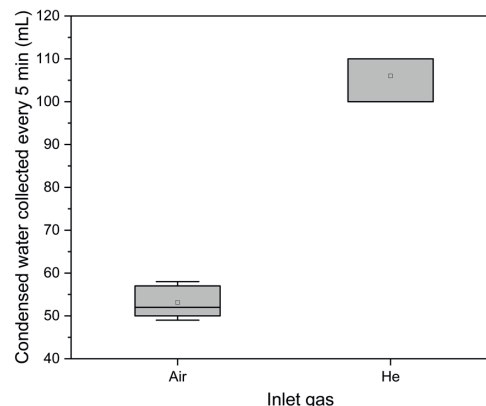


Figure 5. Average volume of condensed water collected every 5 minutes from the NaCl solution with the inlet gas air or helium at 54°C.

To enable a comparison between air and helium as inlet gases, the inlet-gas temperature was adjusted to achieve the same steady-state solution temperature in the HBPP. The theoretical evaporation rate at the steady-state solution temperature was calculated by multiplying the equilibrium water-vapour density (g/m^3) by the corresponding flow rate. As the rotary gas meter used to measure the helium flowrate was also used to measure the flow rate of air, a correction factor for the flow rate was needed. The flow rate of air produced using the two air blowers (Hiblow HP 120) was measured by the rotary gas meter (FMR DN40 G016) as 260 L/min. The flow rate of air into the solution was measured by the meter at about 150 L/min.

It is well known that data for equilibrium water vapour density as a function of liquid water temperature is the same for all gases, including helium and air¹⁴. Thus, the saturated water-vapour density in a helium atmosphere matches that in an air bubble at the same solution temperature. As a result, the theoretical amount of water vapour collected using the same flow rate is the same for both air and helium.

This equivalence allowed a direct comparison of the water-vapour collection performance of the two gases at the same steady-state solution temperature. The volume of condensed water collected was multiplied by the specific heat capacity of each gas to calculate the relative evaporation efficiency of $H(T_e)$ of helium and dry air at an equilibrium temperature T_e using

$$H(T_e) = \frac{V_h}{V_a} \times \frac{C_p(\text{air})}{C_p(\text{He})}$$

where V_h and V_a are the average volumes of water produced (mL) over the 5-minute periods at the temperature T_e (K) using helium and dry air, respectively, and $C_p(\text{air})$ and $C_p(\text{He})$ are the corresponding specific heat capacities (J/molK) at this temperature.

At around 54°C, the HBPP using helium achieved an evaporation efficiency 2.8 times higher than that of air (Table 3).

Table 3. Relative evaporation efficiency, helium vs dry air.

Equilibrium temp./°C		Condensed water vapour/mL		Relative evaporation efficiency He/Air
Air	He	Air	He	
53.7	53.5	53.1	106	2.8

Note: Condensed water vapour is the average amount collected every 5 minutes in a 60-minute run. The relative evaporation efficiency was calculated from Equation (1) with the specific heat capacity of air 29.2 J/molK, and of helium 20.8 J/molK.

These results align with those reported by ^{5,14} for a lab-scale BCE sparged with dry air or helium into an aqueous solution at a solution temperature of either 25°C¹⁴ (3.1 times) or 45°C⁵ (3.3 times). The difference in evaporation efficiency may be attributed to the inefficiency in condensing the water vapour collected in the larger-scale HBPP.

The improved evaporation efficiency with helium was further confirmed using statistical analysis. The evaporation efficiency for both gases was found to follow a normal distribution at 54°C, so the independent t -test was used. The null hypothesis assumed that the evaporation efficiency remains the same, regardless of the type of gas used, whereas the alternative hypothesis was that the evaporation efficiency is different for each gas. The analysis provided strong evidence (95% CL) that the efficiency of evaporation was higher with helium than with air at 54°C ($t = -14.8$, $df = 5.59$, $p < 0.0001$), which agreed well with results obtained from a laboratory-scale BCE^{5,14}.

According to Wei and Pashley¹⁴, the superior performance of helium as an inlet gas can be attributed to its small molecular size and stable atomic configuration. Its smaller molecular size allows for greater penetration into the water surrounding the bubbles compared to larger air molecules. Evidence for this has been shown in²¹. This greater penetration disrupts the local hydrogen bonds, aiding evaporation^{5,14}. Helium's atomic structure might also enable it to trap gas-phase water molecules in its lattice structures over a wide range of pressures

and temperatures, thereby promoting enhanced evaporation at lower temperatures and reducing the thermal energy needed for desalination²⁵. Additionally, the superior thermal conductivity of helium increases the heat-transfer coefficient, further enhancing the evaporation process¹⁴. Wei and Pashley¹⁴ pointed out that bubbles produced with helium have a higher density than air bubbles at the same flowrate. The formation of more and finer bubbles, along with the inhibition of bubble coalescence by the salt in the column solution, enhances the rate of heat and mass transfer between the hot bubbles and the solution, thereby increasing the evaporation rate of water molecules.

Energy consumption

In the context of large-scale desalination using the HBPP, energy consumption is also an important factor to assess the efficiency of the process. Hence, an estimate of the energy using helium in the HBPP for desalination at an equilibrium solution temperature of 54°C was calculated as follows.

The specific heat capacity per unit weight of helium gas $C_p^g(\text{He}) = 5.19 \text{ J/gK}$ or 20.8 J/molK . Helium at 147°C gave an equilibrium solution temperature of about 54°C with a relative evaporation efficiency compared to air, of about 3 (Table 1).

Consider a helium bubble with an average diameter of 1.5 mm. Assuming it to be spherical, the average volume can be found using the standard formula

$$V = \frac{4 \times \pi}{3} \times \left(\frac{1.5 \text{ mm}}{2}\right)^3 = 1.77 \text{ mm}^3 = 1.77 \times 10^{-9} \text{ m}^3$$

The average mass of helium bubble therefore will be (considering a density of 0.178 kg/m^3) =

$$1.77 \times 10^{-9} \text{ m}^3 \times 0.178 \frac{\text{kg}}{\text{m}^3} = 3.16 \times 10^{-7} \text{ g}$$

- a rough estimate for a mm-sized helium bubble in water. Next, the volume of a helium bubble leaving the top of the reactor at 54°C = 327 K was calculated using:

$$V' = \frac{nRT_e}{P} = \frac{\frac{3.16 \times 10^{-7} \text{ g}}{4 \frac{\text{g}}{\text{mol}}} \times \frac{8.314 \text{ J}}{\text{K.mol}} \times 327 \text{ K}}{1 \text{ atm} \times 10^5 \frac{\text{Pa}}{\text{atm}}} = 2.15 \times 10^{-9} \text{ m}^3$$

The amount of heat (and work) required to heat this volume of helium is given by the difference between room temperature (around 20°C) and the inlet helium temperature (around 147°C) multiplied by the specific heat capacity of helium (5.19 J/gK)⁵, that is,

$$[C_p^g(\text{He}) \times m_{\text{He}} \times \Delta T] = 5.19 \text{ J/gK} \times 3.16 \times 10^{-7} \text{ g} \times (147 - 20) \text{ K} = 2.08 \times 10^{-4} \text{ J}.$$

At this temperature, the saturated water-vapour density carried in a bubble of any gas, $\rho_v(T_e)$ is about 101.9 g/m^3 ⁵. Therefore, the total amount of water vapour transferred into the helium bubble is

$$101.9 \text{ g/m}^3 \times 2.15 \times 10^{-9} \text{ m}^3 = 2.19 \times 10^{-7} \text{ g}.$$

As observed in this current work, there was a 1.5 times increase in water vapour produced with helium at 54°C compared to the theoretical water-vaporisation rate (Table 2) for 1000 L of condensed water recovered from the saline solution (0.5 M NaCl) in HBPP; the process therefore requires:

$$\frac{1000 \text{ L} \times 10^3 \text{ g/L}}{2.19 \times 10^{-7} \text{ g} \times 1.5} \times 2.08 \times 10^{-4} \text{ J} = 6.33 \times 10^8 \text{ J}$$

that is 1 kL of condensed water is 633 MJ/kL, which is the energy cost per kL of water produced by using helium at 54°C within HBPP.

It is very important to use solar heating to preheat the seawater and thus making the bubble vapour desalination process viable and competitive with MSF, in terms of the energy demand. By comparison, the highest-energy-consuming commercial boiling method uses 67 kWh/m^3 or about 240 MJ/kL ($1 \text{ kWh} = 3.6 \text{ MJ}$)²⁶. Furthermore, the thermal-energy recovery such as that used in multi-stage flash distillation reduces the energy demand by over 90%, to values as low as 100 MJ/kL ²⁶. In comparison, most of the energy demand (633 MJ/kL) calculated for the HBPP/He method is not, currently, recycled on condensation of the water vapour, and is not used to heat the saltwater feed.

Overall, present results show that although there is an improved helium carryover of water vapour compared with a dry air inlet at the same equilibrium temperature, the energy required to evaporate the same amount of water calculated for helium achieved by HBPP is higher than that required in the worst commercial boiling method²⁶. Hence, the HBPP/He method could only be viable with thermal-energy recovery or by using solar heating.

3.2.2 Combustion gas, helium and air

Figure 6 shows the volumes of condensed water collected using dry air, combustion gas or helium as the inlet gas, all at 90°C .

Combustion gas produced the largest amount of condensed water, followed by helium and air ($F = 81.49$; $df(2, 33)$; $p < 0.0001$; Dunnett T3 test, 95% CL), in agreement with previous studies^{16,19}. This was, at least in part, because of the amount of water vapour in the combustion gas, calculated using Equation (2).

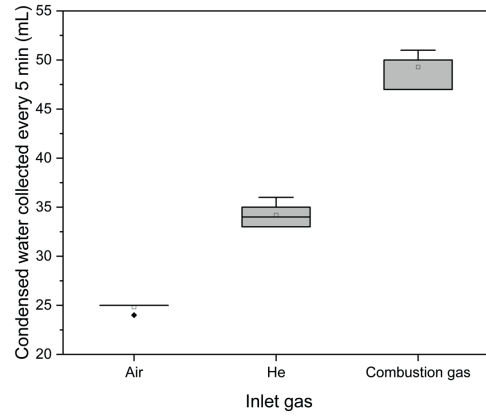
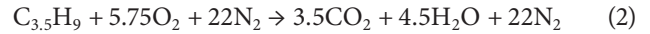


Figure 6. Average volume of condensed water collected every 5 minutes from the NaCl solution with dry air, combustion gas or helium, all at an inlet temperature of 90°C .

In this work, the combustion gas was produced by the combustion of LPG ($\text{C}_{3.5}\text{H}_9$) in the gas generator without additional heating¹⁹:



Equation 2 shows that water vapour is produced in the combustion process and is therefore present in the inlet gas. As a result, when the net amount of water vapour evaporated was calculated, this extra water vapour had to be taken into account.

Additionally, with combustion gas as the inlet gas, the total energy heat transferred by the gas bubbles includes the exothermic heat from the hot water vapour in the combustion gas¹⁹. That is to say that the hot inlet combustion gases do not use the heat to evaporate pre-existing water vapour as they already come with a great percentage of hot water vapour, making it greater than the heat supplied by the other heated gases. The condensation of this water vapour releases additional heat to evaporate the column solution¹⁹:

$$Q_w + \Delta T' \times C_p(T_e) + \Delta p = \rho_v(T_e) \times \Delta H_v(T_e) \quad (3)$$

Here, Q_w (J/m^3) is the exothermic heat transferred from the water vapour contained in the combustion gas inlet but has not been used to evaporate the solution; $C_p(T_e)$ ($\text{J/m}^3\text{K}$) is the specific heat capacity of the inlet gas at the equilibrium solution temperature; $\Delta T'$ (K) is the temperature difference between the gas entering and the gas leaving the column; Δp (J/m^3) is the hydrostatic pressure difference between the inlet gas flow and the atmosphere. The term $\rho_v(T_e)$ (mol/m^3) on the right-hand side is the vapour density at the equilibrium solution tempera-

ture and $\Delta H_v(T_e)$ (J/mol) is the enthalpy of vaporisation of the column solution. Equation (3) shows that, with combustion gas as the inlet gas, the calculation of the total heat transferred by the gas bubbles must take into account the heat released from the water vapour in the combustion gas¹⁹.

The saturated water-vapour density depends on the solution temperature but not whether the solution is boiling or not¹⁴. A higher equilibrium temperature of the water in the reactor was observed for combustion gas compared to helium and air (Fig. 6). Furthermore, since the inlet combustion gas contained hot water vapour, CO_2 and N_2 (Equation (2)), it had more degrees of freedom and a higher heat capacity, which resulted in a column-solution temperature (56°C) higher than helium (40°C), a less complex gas molecule (Fig. 7).

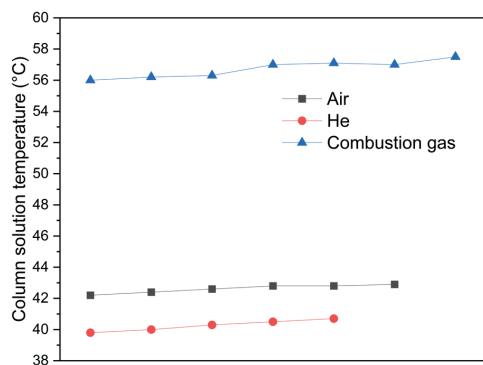


Figure 7. Temperature of the NaCl solution every 5 minutes with the inlet gas air, combustion gas or helium, all at 90°C .

Additionally, due to the exothermic liquefaction reaction of the hot water vapour contained in the combustion gas (Equation 2), a higher column solution temperature was achieved with combustion gas (56°C) compared to dry air (43°C) (Fig. 7). This exothermic heat energy can be determined from the heat released during the condensation of vapour to liquid at 90°C and the subsequent cooling of the 90°C liquid water to 56°C in the column solution (Fig. 7), as shown in¹⁹. Furthermore, since the combustion gas temperature (90°C) was similar to that of the other gases, no additional heating was required.

Hence, using combustion gas as the inlet gas in the HBPP offers two advantages: first, it leverages the high heat capacity of the heated water vapour it contains, enhancing heat transfer between the hot combustion gas bubbles and the solution; second, it utilizes the heat generated by the combustion process to evaporate the solution without requiring additional heating.

Furthermore, the utilization of combustion gas in a single-stage bubble column desalination process at a relatively low temperature would be a viable option compared with the typical multiple-effect evaporation system operating under vacuum. By comparison, a multiple-effect evaporation system operating under vacuum heats saltwater under a reduced pressure to depress the boiling point, and then a small proportion of water vapour is boiled off and condensed in a series of 'multi stages' process. Substantial energy is required to initiate boiling of the saltwater feed. However, the nature of the bubble vapour desalination process itself means that there is no need to boil the water. In this process, the water vapour content immersed and equilibrated in the bubbles at temperatures significantly below the boiling point is almost identical to that in bubbles carried over by boiling at the same temperature. Furthermore, the water vapour is not only collected on the surface of the liquid as used in the multiple-effect evaporation but is transferred throughout the entire body of the salt solution. Hence, the bubble vapour desalination is a more effective method in terms of energy requirements and is viable when combined with an available source of waste industrial heat, such as from pig farms. The results obtained in this study on the enhanced water recovery with combustion gas are in agreement with those reported by^{16,19}.

Latent heat of vaporization of water

To further understand the mechanism by which combustion gas enhances water evaporation efficiency in the desalination process of the HBPP large-scale pilot test unit, the latent heat of vaporisation $\Delta H_v(T_e)$ of the column solution was determined in relation to changes in the steady-state equilibration temperature within the combustion gas atmosphere. This was achieved by applying a steady-state thermal energy balance between the combustion gas and the surrounding salt solution, assuming that the vapour pressure of water at this temperature is known. It should be noted that in this energy balance, the $\Delta H_v(T_e)$ term accounts for the expansion of bubbles as they absorb water vapour, while the corresponding reduction in gas volume is represented by the $C_p(T_e)$ term²⁴.

By using the same steady state thermal energy balance developed in a bubble vapour desalination process, the calculated results of the enthalpy of water vaporization (ΔH_v) in an aqueous salt solution sparged by other input carrier gases (dry air and helium) have been reported and are shown in Table 4. In this energy balance formula, only the steady state equilibration tem-

perature of the bubble column, temperature of the inlet gas and the hydrostatic pressure across the column need to be measured to determine the heat of vaporization for water.

Regarding the use of combustion gas, assuming that 1 mol of combustion gas ($C_{3.5}H_9$) consists of a mixture of 3.5 mol CO_2 , 4.5 mol H_2O , and 22 mol N_2 (Equation 3), the specific heat capacity per unit weight of the combustion gas at the reactor's equilibrium temperature is given by

$$C_p^g(T_e) = \frac{n_{CO_2}M_{CO_2}c_p(CO_2) + n_{H_2O}M_{H_2O}c_p(H_2O) + n_{N_2}M_{N_2}c_p(N_2)}{m_{CO_2} + m_{H_2O} + m_{N_2}} =$$

$$\frac{3.5 \text{ moles} \times 44 \frac{\text{g}}{\text{mol}} \times \frac{0.844 \text{ J}}{\text{g} \cdot \text{K}} + 4.5 \text{ moles} \times 18 \frac{\text{g}}{\text{mol}} \times \frac{4.18 \text{ J}}{\text{g} \cdot \text{K}} + 22 \text{ moles} \times 28 \frac{\text{g}}{\text{mol}} \times \frac{1.040 \text{ J}}{\text{g} \cdot \text{K}}}{3.5 \text{ moles} \times 44 \frac{\text{g}}{\text{mol}} + 4.5 \text{ moles} \times 18 \frac{\text{g}}{\text{mol}} + 22 \text{ moles} \times 28 \frac{\text{g}}{\text{mol}}} = 1.3 \text{ J/gK}.$$

This value remained fairly constant over a wide temperature range of 0–100°C. It must be converted into the heat per unit volume of combustion gas released from the reactor, $C_p(T_e)$, expressed in units of J/m³K.

The specific heat of combustion gas $C_p(T_e)$, in units of J/m³K is given by the specific heat per unit weight of combustion gas $C_p(T_e)$, in units of J/gK multiplied by the vapour density carried in the combustion gas mixture at equilibrium $\bar{\rho}_v$, in units of g/m³.

To calculate the vapour density $\bar{\rho}_v$, the molar mass (M) of the combustion gas mixture is calculated using the mole of gas compositions in mixture, that is

$$M = \frac{3.5 \text{ moles} \times 44 \frac{\text{g}}{\text{mol}} + 4.5 \text{ moles} \times 18 \frac{\text{g}}{\text{mol}} + 22 \text{ moles} \times 28 \frac{\text{g}}{\text{mol}}}{3.5 \text{ moles} + 4.5 \text{ moles} + 22 \text{ moles}} = 28.37 \frac{\text{g}}{\text{mol}}$$

Using the ideal gas equation, the vapour density carried in the combustion gas $\bar{\rho}_v$ is given below:

$$\bar{\rho}_v = \frac{PM}{RT_e} = \frac{101325 \frac{\text{J}}{\text{m}^3} \times 28.37 \frac{\text{g}}{\text{mol}}}{8.314 \frac{\text{J}}{\text{mol} \cdot \text{K}} \times (56 + 273.15) \text{ K}} = 1050.32 \text{ g/m}^3$$

This converts the heat capacity per unit weight of combustion gas mixture to the heat capacity per unit volume:

$$C_p(T_e) = C_p^g(T_e) \times \bar{\rho}_v = 1.3 \text{ J/gK} \times 1050.32 \text{ g/m}^3 = 1365.416 \text{ J/m}^3\text{K}.$$

The saturated water vapour density, $\rho_v(T_e)$, at equilibrium is provided in references ^{4,5}. At a column temperature of approximately 56°C, its value is 112 g/m³. Assuming no pressure difference in the combustion gas between the point just before it entered the sinter and the atmospheric pressure at which it passed through the reactor, the hydrostatic pressure difference across the sinter and water column would be $\Delta P = 0 \text{ J/m}^3$.

This assumption is reasonable, as the HBPP operates under atmospheric pressure conditions. These calculated

values were used to determine the enthalpy of vaporisation of water with combustion gas inlet, given by

$$\Delta H_v(T_e) = \frac{\Delta T \times C_p(T_e)}{\rho_v(T_e)} = \frac{(90 - 56) \text{ K} \times 1365.416 \frac{\text{J}}{\text{m}^3\text{K}}}{112 \frac{\text{g}}{\text{m}^3}} =$$

$$414.50 \text{ J/g (or 7.46 kJ/mol)}$$

at a column temperature of around 56°C. In the bubble column reactor, the corresponding values of ΔH_v in a helium or air atmosphere are approximately 15.50 kJ/mol and 13.75 kJ/mol, respectively, when the HBPP operates at steady-state equilibration temperatures of 40°C and 43°C (Table 4).

Table 4. Calculated heat of vaporization using the energy balance formula

Inlet gas	Air	Helium	Combustion gas
T_e (°C)	43	40	56
$C_p(T_e)$ (J/gK)	1.0	5.19	1.3
$\rho_v(T_e)$ (g/m ³)	61.0	52.97	112
$\Delta H_v(T_e)$ (kJ/mol)	15.50	13.75	7.46

A significant drop in the calculated ΔH_v values correlated with the observation of an increased condensation efficiency of water vapor from the salt solution suggest that the use of combustion gas as inlet gas within HBPP can facilitate the evaporation process more promising than helium. The decreased effective value of ΔH_v reported for the HBPP sparged with pre-heated helium inlet gases into the aqueous salt solution also indicates the superior performance of helium in decreasing the energy required at promoting the evaporation of the same amount of water via the mechanism proposed, compared with dry air.

Overall, the ΔH_v values obtained for different inlet gases sparging under equilibrium column conditions confirm that heated combustion gas significantly enhances the efficiency of water evaporation in the HBPP. This improved performance is likely due to a reduction in the effective value of ΔH_v for water.

4. CONCLUSIONS

The HBPP was developed as a small-scale industrial implementation of the BCE method. Three different gases were used for the inlet gas. Increased inlet-gas temperatures resulted in increased evaporation efficiency, primarily due to the increased heat transfer from the gas bubbles.

The HBPP performed better with helium as the inlet gas than with dry air at a solution temperature of 54°C; the evaporation efficiency with helium was 3 times greater than with air, similar to that observed with helium in a

laboratory-scale BCE at solution temperatures of either 25°C ¹⁴ or 45°C ⁵. The HBPP achieved the energy consumption using helium at a solution temperature of 54°C of around 633 MJ/kL and could only be competitive with thermal-energy recovery or the use of solar energy because even in the commercial boiling method using the most energy (MSF), the energy demand can be reduced by over 90 % to 240 MJ/kL using energy recovery.

Combustion gas at 90°C produced a greater amount of condensed water vapour in the HBPP than helium and dry air, without requiring additional heating. The enthalpy of water vaporisation in a combustion gas-sparged aqueous solution was calculated using the energy balance equation for an upscaled BCE system. These findings suggest that the HBPP holds potential for development into a simple and efficient commercial seawater desalination process, particularly when utilizing gases derived from the combustion of waste materials.

CRediT authorship contribution statement

Thi Thuy Nguyen: Conceptualization, investigation, data curation, formal analysis, methodology, writing – original draft, writing – review editing. **Adrian Garrido Sanchis:** Conceptualization, investigation, supervision, writing – review editing, funding acquisition. **Richard M. Pashley:** Supervision, writing – review editing.

Declaration of competing interest

The authors declare that they do not possess any identifiable financial conflicts of interest or personal relationships that might have appeared to impact the findings presented in this paper.

Data availability: Data will be made available on request.

Acknowledgements

This study was funded by Australian Pork Limited (APL), grant number APL2018/0074. Dr. Peter McIntyre is gratefully acknowledged for his assistance in manuscript editing.

REFERENCES

- (1) Khawaji, A. D.; Kutubkhanah, I. K.; Wie, J.-M. Advances in Seawater Desalination Technologies. *Desalination* **2008**, 221 (1–3), 47–69. <https://doi.org/10.1016/j.desal.2007.01.067>.
- (2) Mezher, T.; Fath, H.; Abbas, Z.; Khaled, A. Techno-Economic Assessment and Environmental Impacts of Desalination Technologies. *Desalination* **2011**, 266 (1–3), 263–273. <https://doi.org/10.1016/j.desal.2010.08.035>.
- (3) Shahid, M. A Study of the Bubble Column Evaporator Method for Improved Sterilization. *Journal of Water Process Engineering* **2015**, 8, e1–e6. <https://doi.org/10.1016/J.JWPE.2014.10.009>.
- (4) Shahid, M.; Fan, C.; Pashley, R. M. Insight into the Bubble Column Evaporator and Its Applications. *Int Rev Phys Chem* **2016**, 35 (1), 143–185. <https://doi.org/10.1080/0144235X.2016.1147144>.
- (5) Taseidifar, M.; Shahid, M.; Pashley, R. M. A Study of the Bubble Column Evaporator Method for Improved Thermal Desalination. *Desalination* **2018**, 432, 97–103. <https://doi.org/10.1016/j.desal.2018.01.003>.
- (6) Shahid, M.; Xue, X.; Fan, C.; Ninham, B. W.; Pashley, R. M. Study of a Novel Method for the Thermolysis of Solutes in Aqueous Solution Using a Low Temperature Bubble Column Evaporator. *J Phys Chem B* **2015**, 119 (25), 8072–8079. <https://doi.org/10.1021/acs.jpcc.5b02808>.
- (7) Francis, M. J.; Pashley, R. M. Thermal Desalination Using a Non-Boiling Bubble Column. *Desalination Water Treat* **2009**, 12 (1–3), 155–161. <https://doi.org/10.5004/dwt.2009.917>.
- (8) Shahid, M.; Taseidifar, M.; Pashley, R. M. A Study of the Bubble Column Evaporator Method for Improved Ammonium Bicarbonate Decomposition in Aqueous Solutions: Desalination and Other Techniques. *Substantia* **2021**, 49–55. <https://doi.org/10.36253/Substantia-833>.
- (9) Sanchis, A. G.; Shahid, M.; Pashley, R. M. Improved Virus Inactivation Using a Hot Bubble Column Evaporator (HBCE). *Colloids Surf B Biointerfaces* **2018**, 165, 293–302. <https://doi.org/10.1016/j.col-surfb.2018.02.030>.
- (10) Craig, V. S. J.; Ninham, B. W.; Pashley, R. M. The Effect of Electrolytes on Bubble Coalescence in Water. *J Phys Chem* **1993**, 97 (39), 10192–10197. <https://doi.org/10.1021/j100141a047>.
- (11) Leifer, I.; Patro, R. K.; Bowyer, P. A Study on the Temperature Variation of Rise Velocity for Large Clean Bubbles. *J Atmos Ocean Technol* **2000**, 17 (10), 1392–1402. [https://doi.org/10.1175/1520-0426\(2000\)017<1392:ASOTTV>2.0.CO;2](https://doi.org/10.1175/1520-0426(2000)017<1392:ASOTTV>2.0.CO;2).
- (12) Ninham, B. W.; Pashley, R. M.; Nostro, P. Lo. Surface Forces: Changing Concepts and Complexity with

- Dissolved Gas, Bubbles, Salt and Heat. *Curr Opin Colloid Interface Sci* **2017**, 27, 25–32. <https://doi.org/10.1016/J.COCIS.2016.09.003>.
- (13) Pashley, R. M.; Francis, M. J.; Rzechowicz, M. Unusual Properties of Water: Effects on Desalination Processes. *Water (Basel)* **2008**, 35 (8), 67–71.
- (14) Wei, R.; Pashley, R. M. An Improved Evaporation Process with Helium Inlet in a Bubble Column Evaporator for Seawater Desalination. *Desalination* **2020**, 479, 114329. <https://doi.org/10.1016/j.desal.2020.114329>.
- (15) Ninham, B. W.; Shahid, M.; Pashley, R. M. A Review and Update of Bubble Column Evaporator Processes. *Substantia* **2021**, 4 (2), 19–32. <https://doi.org/10.36253/Substantia-823>.
- (16) Wei, R.; Sanchis, A. G. A New Commercial Prototype of a Bubble Column Evaporator (BCE) for High-Quality Water Production in Livestock (Piggery) Farms. *J Environ Chem Eng* **2023**, 11 (2), 109463. <https://doi.org/10.1016/j.jece.2023.109463>.
- (17) Shahid, M.; Pashley, R. M. A Study of the Bubble Column Evaporator Method for Thermal Desalination. *Desalination* **2014**, 351, 236–242. <https://doi.org/10.1016/j.desal.2014.07.014>.
- (18) Fan, C.; Shahid, M.; Pashley, R. M. The Energy Balance within a Bubble Column Evaporator, Heat and Mass Transfer. *Heat and Mass Transfer* **2018**, 54 (5), 1313–1321. <https://doi.org/10.1007/s00231-017-2234-x>.
- (19) Wei, R.; Sanchis, A. G. The Improved Evaporation Efficiency of a Hot-Bubble Pilot Plant (HBPP) Caused by Combustion Gas for Water Treatment. *Water Resour Ind* **2021**, 25, 100151. <https://doi.org/10.1016/j.wri.2021.100151>.
- (20) Garrido Sanchis, A.; Jin, L. Evaluation of the New Energy-Efficient Hot Bubble Pilot Plant (HBPP) for Water Sterilization from the Livestock Farming Industry. *Water Resour Ind* **2020**, 24, 100135. <https://doi.org/10.1016/j.wri.2020.100135>.
- (21) Wei, R. A Study of the Improved Evaporation Efficiency of a Bubble Column Evaporator for Water Treatment. Thesis, UNSW Canberra, Canberra, 2021. <https://doi.org/https://doi.org/10.26190/unsworks/24050>.
- (22) Bakan, H. I. A Novel Water Leaching and Sintering Process for Manufacturing Highly Porous Stainless Steel. *Scr Mater* **2006**, 55 (2), 203–206. <https://doi.org/10.1016/J.SCRIPTAMAT.2006.03.039>.
- (23) Fan, C.; Shahid, M.; Pashley, R. M. Studies on Bubble Column Evaporation in Various Salt Solutions. *J Solution Chem* **2014**, 43 (8), 1297–1312. <https://doi.org/10.1007/s10953-014-0206-z>.
- (24) Francis, M. J.; Pashley, R. M. Application of a Bubble Column for Evaporative Cooling and a Simple Procedure for Determining the Latent Heat of Vaporization of Aqueous Salt Solutions. *J Phys Chem B* **2009**, 113 (27), 9311–9315. <https://doi.org/10.1021/jp901801k>.
- (25) Prakash Narayan, G.; McGovern, R. K.; Lienhard V, J. H.; Zubair, S. M. Helium as a Carrier Gas in Humidification Dehumidification Desalination Systems. *ASME 2011 International Mechanical Engineering Congress and Exposition, IMECE 2011* **2012**, 1, 437–444. <https://doi.org/10.1115/IMECE2011-62875>.
- (26) Ghazi, Z. M.; Rizvi, S. W. F.; Shahid, W. M.; Abdulhameed, A. M.; Saleem, H.; Zaidi, S. J. An Overview of Water Desalination Systems Integrated with Renewable Energy Sources. *Desalination* **2022**, 542, 116063. <https://doi.org/10.1016/j.desal.2022.116063>.